Production of drug-releasing biodegradable microporous scaffold impregnated with gemcitabine using a CO_2 foaming process

Álvarez, I. [a], Gutiérrez, C. [b], Rodríguez, J.F. [a], de Lucas, A. [a], García, M.T.[a, *]

[a,] Department of Chemical Engineering. University of Castilla-La Mancha. Facultad de C.C. Químicas. Avda. Camilo José Cela 12, 13071 Ciudad Real, Spain.

[b] AMBLING Ingeniería y Servicios. Cáceres, Plasencia, Spain.

[*]Corresponding author:

e-mail: Teresa.García@uclm.es

Phone: +34926295300/5311

Fax: +34926295256

Abstract

The use of supercritical fluids technology, in particular the use of CO_2, is an important advantage over other production techniques of controlled release systems. The impregnation and foaming process can be carried out in a single step. By adjusting the conditions of pressure, temperature, depressurization time or type of polymer used, microcellular scaffolds can be obtained with desired characteristics and adapted to the patient's requirements. In this work, Gemcitabine impregnation in PLGA foams from polymeric solutions of ethyl lactate has been studied. The effect of polymer lactide to glycolide ratio, pressure and temperature were studied for three initial drug loading. In addition, an impregnation efficiency study was performed under these conditions, as well as an Energy Dispersive Spectroscopy analysis (EDS) to determine if Gemcitabine was uniformly distributed throughout the polymeric matrix. Finally, a study of the release profile of Gemcitabine in Phosphate Buffered Saline (PBS) was investigated and a mathematical modelling was carried out. In this model it was considered that the release process was divided into three different steps controlled by the external diffusion in the first place, by the internal transfer of mass in the second and then by the degradation of the polymer.

1. Introduction

Biodegradable polymers derived from lactic acid and glycolic acid have been widely used in medical and pharmaceutical applications [1-8]. Nowadays, interest in foam synthesis of these polymers has increased. The main characteristic that makes the use of these polymers so attractive is that their degradation products are eliminated by the body's metabolic pathways avoiding side effects [9, 10]. Moreover, the use of biodegradable polymers such as Poly (lactic-co-glycolic) acid (PLGA) eliminates a posterior surgery stage to remove traditional implants.

Porous biodegradable foams have been produced for delivery of anticancer drugs and for the regeneration of tissues and organs [11-19]. These porous scaffolds with an open pore structure are also desirable in many tissue engineering applications in order to maximize cell seeding, attachment, growth, extracellular matrix production, vascularization, and tissue growth [20, 21]. Moreover, porous matrices are interesting impregnation supports due to their large specific surface area [22].

Conventional drug delivery products provide sharp increases in drug concentration that can reach toxic levels, followed by a relatively short period at the therapeutic level after which, drug concentration drops until new administration occurs [23]. In contrast, controlled release systems try to achieve release profiles that yield the therapeutic systemic concentration of the drug over a longer period of time, avoiding the large fluctuations in drug concentration and reducing the need for frequent administrations [24].

The use of supercritical carbon dioxide is a technology that allows the foaming and impregnation of polymer matrix with a drug in a single step [25-27]. Supercritical CO_2 assisted impregnation has proven to be feasible when pharmaceutical compound is soluble in carbon dioxide and the polymer can be swollen by the supercritical fluid [28]. This impregnation process of active compounds in polymeric matrices is very complex and is subject to the interactions that may occur between the solute (active principle), the carrier (supercritical fluid and modifier) and the polymeric matrix [29].

Gemcitabine is a pyrimidine analogue and has demonstrated antitumor activity in a variety of solid tumors of bladder, lung, ovary and pancreas [30-33]. This drug possesses radiosensitizing properties *in vitro* and *in vivo* at non-cytotoxic concentrations. Currently, Gemcitabine is used as the single agent for the treatment of advanced pancreatic cancer and is the most widely prescribed cancer drug worldwide [6, 34-42], but a high dose of drug is required to achieve the therapeutic concentration or desired effect, causing serious side effects.

In this work, the impregnation of Gemcitabine in PLGA polymeric matrices by means of supercritical technology and further release kinetics has been studied. The degradation rate of the scaffold should be similar to or slower than the rate of drug absorption for the organism. Consequently, it is important to understand the degradation profile of a given polymer scaffold. Because of that, a mathematical model has been developed in order to describe the release profile of Gemcitabine at three different concentrations in the PLGA matrix. The influence of Gemcitabine concentration on the final structure of the microcellular foam, as well as the working pressure, temperature and PLA to PGA ratio has also been investigated.

2. Materials

2.1. Materials

Poly (lactic-co-glycolic) acid (PLGA) with different ratio lactide:glycolide (average molecular weight 17,000 g/mol) was used for the synthesis of the microparticles. PLGA5050 (50 mol % lactic acid, 50 mol % glycolic acid) and PLGA7525 (75 mol % lactic acid, 25 mol % glycolic acid) were supplied by Corbion Purac (Netherlands) and used as received. Ethyl lactate was acquired from Sigma-Aldrich (Spain) and used as received. Gemcitabine hydrochloride was also supplied by Sigma-Aldrich (Spain). Carbon dioxide with a purity of 99.8% was supplied by Carburos Metálicos S.A. (Spain).

2.2. Experimental impregnation setup and procedure

Impregnation experiments were carried out in a homemade batch-type device consisting of a 316-stainless-steel high-pressure vessel with a volume of 350 mL. To impregnate and foam PLGA solutions, firstly, a solution of 0.8 g PLGA/ml ethyl lactate was prepared. The corresponding amount of drug was added into the solution and homogenized for 5 minutes with a CAT Undrive X 1000 D homogenizer at 5600 rpm. 0.2 gram of the dispersion was placed in a 16 mm diameter support inside the vessel. The vessel was then filled with high-pressure CO_2, which was cooled and compressed by the positive-displacement pump. The pressure was regulated by a back-pressure regulator (BPR) and checked by a manometer. Temperature and pressure were kept constant for 24 hours to promote the formation of a homogeneous microcellular structure because of CO_2 sorption and the solubilization of the solvent in the gas phase. Then, the vessel was vented by opening the discharge valve that was controlled manually by the measurement of the flow in the turbine flow meter.

2.3. Foam characterization

a) Foams structure and internal morphology

Cell structure and morphology were studied by scanning electron microscopy (SEM) using a Quanta 250 equipment with a wolfram filament operating at a working potential of 10 kV (FEI Company). Motic Images 2.0 software was used to analyse mean cell size and homogeneity calculated from the standard deviation of the sample based on the SEM images. Also, cell density was determined, that is defined as the number of cells of foamed sample per unit volume of the original polymer and was calculated according to the following expression:

$$Cells\ density\ \left(\frac{cells}{cm^3}\right) = \left(\frac{n \cdot M^2}{A}\right)^{3/2} \quad (1)$$

where n is the number of cells in the micrograph, A the area of the micrograph (cm^2) and M the magnification factor [43, 44].

105 An Energy Dispersive Spectroscopy (EDS) analysis was performed in order to know if
106 the drug was homogeneously distributed through all the foam. The apparatus used was an analysis
107 system coupled to the SEM equipment.
108

109 **b) Thermal analysis**

110 The residual amount of solvent and the presence of Gemcitabine was further confirmed
111 by thermogravimetric analysis TA-DSC Q 600. Weight loss due to solvent volatilization (~150
112 °C), Gemcitabine degradation (~280 °C) and polymer degradation (~ 325 °C) was recorded in the
113 thermograph as a function of temperature. DSC scans were done using a DSC Q1000 TA. DSC
114 analysis were performed to stablish the glass transition temperature of PLGA flakes and PLGA
115 impregnated foams. The data were analysed with the universal analysis software TA 2000.
116

117 **c) FTIR analysis**

118 The FTIR spectra of PLGA polymer, PLGA foams, Gemcitabine and PLGA impregnated
119 foams were recorded on a JASCO FT/IR 4600. It was used for chemical analyses of the functional
120 groups present in microparticles. IR spectra of microparticles samples were obtained in range
121 from 4000 cm^{-1} to 400 cm^{-1}, with a resolution of 4.0 cm^{-1} and 64 scanning.
122

123 ## 2.4. *In vitro* release experiments

124 About 100 mg of Gemcitabine impregnated foams was introduced into 100 mL of
125 Phosphate Buffered Saline (PBS) in hermetically sealed glass bottles protected from light (Figure
126 3.5). These bottles were placed in a water-bath at 37 °C to simulate body temperature and were
127 kept agitated during this analysis. A sample of 2 mL from the solution was drawn for each
128 established time, at 1h, 3h, 6h, and 24h. After this point, the sample was measured every day until
129 day 22. The experiments were duplicated. In order to maintain the origin PBS volume and pH
130 value, 2 mL of fresh PBS was periodically added until the end of the experiment.

2.5. *In vitro* drug release kinetics: theoretical mechanism

The mechanism of controlled drug release was previously demonstrated by our research group and was described elsewhere [45]. It can be explained following three different steps:

i) Initial burst of drug release in which the most accessible drug impregnated on the surface or in larger pores, in direct contact with the medium, is released as a function of solubility of drug in the medium. Consequently, the gradient in the drug concentration represent the driving force in the mass transfer process in which the external mass transfer coefficient (k_{ext}) is the most characteristic parameter.

ii) Once the most accessible drug has been released, the diffusion of the drug from the bead matrix trough the polymer chains network control the mass transfer process. Graphically, a drastic change in the shape of the release profile is observed.

iii) Finally, the drug that has been entrapped in the polymer network without mobility or time enough to be released can be liberated when the water hydrolyses the polymer into soluble oligomeric and monomeric products. Drug is released progressively because of the polymer degradation until complete polymer solubilization.

2.6. Mathematical modelling

A mathematical model was developed for each of the drug release steps. This model allows the experimental data to be fitted with great precision according to the release mechanisms previously proposed. Table 1 shows the established time values that mark the beginning and end of each of the steps and that have been applied to the model.

Table 1. Initial and final time values for the three steps of the model.

step	t_0	t_f
1st step	t_0^{ext} (0 days)	t_f^{ext} (1 day)
2nd step	t_0^{int} (1 day)	t_f^{int} (5 days)
3rd step	t_0^{deg} (5 days)	t_f^{deg} (∞ = 22 days)

156

157 **i) Release of the most accessible drug**

158 In the first stage of drug release, the most accessible drug was released. This drug was
159 mainly found on the surface of the foam. This first moment of the release was physically observed
160 as a direct dissolution of the drug in the PBS. This process was only controlled by the diffusion
161 in the film. The equation that can be applied to model this stage was the one proposed by Boyd
162 [46] based on a "Thin Film Diffusion Model" (2):

163 $$(1 - F) = -k_{ext} \cdot t \quad (2)$$

164

165 where F is the fractional attainment of equilibrium (it corresponds to M_t/M_∞, where M_t and M_∞,
166 denote the absolute cumulative amounts of drug released at any time t and at infinite, respectively)
167 and k_{ext} is the external mass transfer coefficient. Experimentally, the linear tendency was observed
168 in all experiments until 1 day. Consequently, this first pattern of the release profile was modelling
169 using this diffusion equation.

170

171 **ii) Release of the most inaccessible drug**

172 The second step involved the release of the drug that was impregnated within the
173 polymeric matrix. This process was controlled by the internal diffusion of the drug giving rise to
174 the second zone of the release curves. This intra-porous diffusion was described by Crank [47]
175 using the "Fick's Second Law of Diffusion". Microcellular foams impregnated with Gemcitabine
176 can be considered spherical, so mathematical analysis was based on this geography. The following
177 conditions were considered based on the experimental results for the fit to the model:

178 a) The drug was homogeneously distributed throughout the foam at $t = t_f^{ext} = t_0^{int}$.
179 b) The initial drug concentration was below the solubility of the drug, which was also known
180 as molecular dispersion or monolithic solution. The driving force was very high at any
181 time during the experiment. The approximation of infinite dilution was accepted.
182 c) There was no drug accumulation at the surface of the foam. The rate at which the drug
183 left the device was always equal to the rate at which the drug was brought to the surface
184 by internal diffusion.

d) Perfect sink conditions were provided throughout the experiment.

Considering these premises, the total amount of diffusing substance entering of leaving the sphere was given by equation (3):

$$\frac{M_t}{M_\infty} = 1 - \frac{6}{\pi^2} \sum_{n=1}^{\infty} \frac{1}{n^2} \cdot \exp\left(-\frac{n^2 \cdot \pi^2}{R_0^2} \cdot D \cdot t\right) \quad (3)$$

where R_0 is the characteristic length of spherical foam radius (0.8 cm) and D represents the apparent diffusion coefficient considering homogeneous particle (the existence of "micropores" would not affect the convenience of using this equation) and t is the release time for each measurement.

iii) Degradation of the foam substrate and release of the remaining drug

Once the drug has been mostly released into the medium, it is assumed that the rest of the drug is released due to degradation of the polymeric matrix. This drug could not be released into the medium well mainly because it is embedded in the polymer chains. So that the physical picture of this part is that the mass of drug discharged in this final part of the experiments is entirely related to the polymer degradation, that is, as we consider that the drug is homogeneously distributed into the polymer probe, the release of drug is directly and proportionally related with the polymer degradation. It is also assumed that the diffusion release is very low compared to the degradation of the polymer. Consequently, quantifying the mass loss of each probe and knowing their individual drug loading it is possible to determinate the theoretical drug released to the medium and compare it with the experimental results. The "Shrinking Core Model" outlined by Levenspiel [48] and showed in equation 4, due to it assumes a first order kinetics analogously to the pseudo-first kinetics of the degradation of PLGA:

$$\left(\frac{M_f}{M_0}\right)^{1/3} = 1 - \frac{k_{deg}}{R_0} \quad (4)$$

211

212 where M_0 and M_f represent the mass (foam together with drug) at the beginning of the final part
213 of the release curve ($t_f^{inf} = t_0^{deg} = 5$ days) and at the end of the experiment respectively, R_0 is the
214 initial radius of the spherical foam (0.8 cm) and k_{deg} is the pseudo-first kinetic constant of
215 degradation for the PLGA foam. M_f was directly weighting at the end of the experiment after a
216 drying stage in a vacuum desiccator.

217 Taking into account all the previous information, global model parameters are as follows:

218 i) Zone I: external mass transfer coefficient (k_{ext}).

219 ii) Zone II: effective diffusion coefficient (D).

220 iii) Zone III: pseudo-first kinetic constant of polymer degradation (k_{deg}).

221

222 3. Results

223 3.1. Gemcitabine impregnation experiments

224 In foaming processes, numerous parameters can be modified to tailor the properties of the
225 foams. For this reason, a study of the effect of pressure, temperature and copolymer type has been
226 carried out to investigate the variation in cell diameter, distribution and cell density of the PLGA
227 foams. In addition, it was analysed if a variation of the amount of Gemcitabine in the foams had
228 a significant effect on the final foam structure and the impregnation efficiency. The variables
229 analysed (ratio PLA:PGA, pressure and temperature) were studied in two different levels as
230 summarised Table 2.

231

232 Table 2. Different factors and levels studied in the impregnation experiments. Same factors were
233 considered for the three amounts of Gemcitabine.

Factors	Level 1	Level 2
Ratio PLA:PGA	50:50	75:25
Pressure (bar)	120	200
Temperature (°C)	25	40

234

235 The dose of Gemcitabine impregnated in each foam was estimated on the basis of the
236 weight and body surface of male rats. The body surface of these animals is approximately 0.03
237 m^2 [49]. The single dose of intraperitoneal Gemcitabine pancreas is 1000 mg/m^2 in humans [50,
238 51]. In rats, doses of Gemcitabine have been used in a single treatment cycle of 333 mg/m^2
239 administered on days 0, 3, 6, 9 and 12 by intraperitoneal injection [52]. In this case, the total dose
240 received in the single cycle was 1665 mg/m^2. Thus, according to these data, a total dose of
241 Gemcitabine between 30 mg and 50 mg peritoneal route could be administered to the animals.
242 Based on these parameters and taking into account the external volume and weight of foams, the
243 amount of Gemcitabine to incorporate in the polymeric matrix was 175 mg Gemcitabine/g PLGA.
244 In a further step, the impregnation and release study was performed for two lower concentrations
245 that were within the permitted dose at 105 mg Gemcitabine/g PLGA and 35 mg Gemcitabine/g
246 PLGA.
247
248 **a) Foam structure analysis**
249 Table 3 illustrates the runs carried out for the three Gemcitabine concentrations. The
250 influence of the ratio PLA to PGA, the pressure and the temperature on the cell size, the standard
251 deviation and cell size was studied. All the experiments were performed with a contact time inside
252 the vessel of 24 hours and 30 minutes of depressurization time. They were also carried out under
253 randomness criterion and run out in duplicate.
254
255
256
257
258
259
260
261
262

Table 3. Runs, experimental impregnation conditions, SEM imagess, cells diameter, standard deviations and cells density.

Run	Gemcitabine (mg GEM/ g PLGA)	Ratio PLA:PGA	Pres. (bar)	Temp. (°C)	SEM images 100x	SEM images 200x	Cell diameter (µm)	Stand. Deviation (µm)	Cell density (cells/cm³)
1	175	5050	120	25	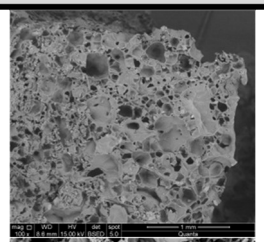	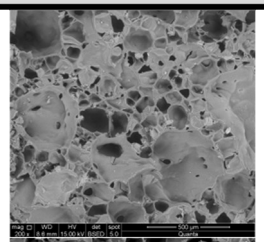	109.20	97.02	1.31E+06
2	175	5050	200	25	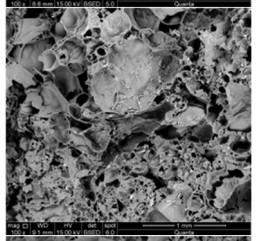	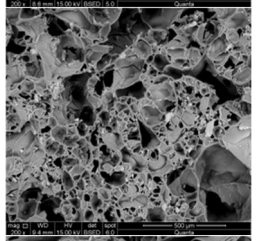	117.25	165.61	2.37E+06
3	175	5050	120	40	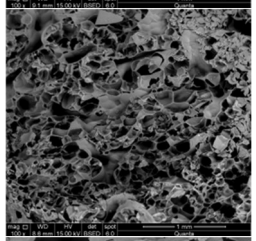	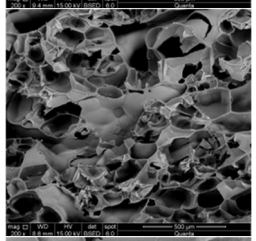	142.46	120.14	1.92E+05
4	175	5050	200	40	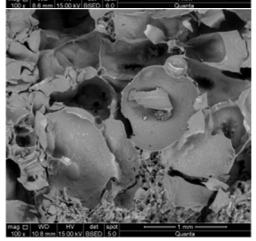	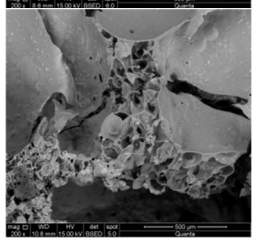	Non homogeneous foam		

Table 3 (cont.). Runs, experimental impregnation conditions, SEM imagess, cells diameter, standard deviations and cells density.

Run	Gemcitabine (mg GEM/ g PLGA)	Ratio PLA:PGA	Pres. (bar)	Temp. (°C)	SEM images 100x	SEM images 200x	Cell diameter (µm)	Stand. Deviation (µm)	Cell density (cells/cm³)
5	175	7525	120	25	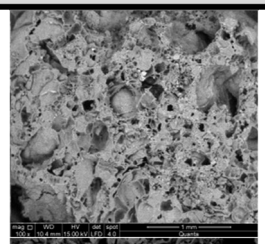	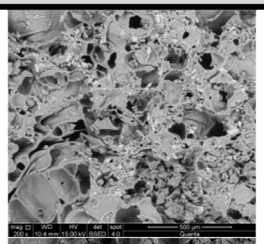	97.58	110.22	3.02E+06
6	175	7525	200	25	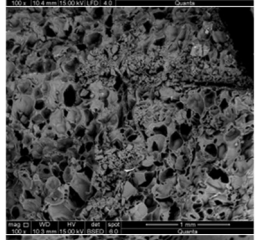	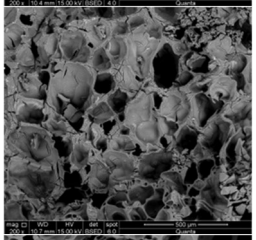	144.38	83.91	7.59E+05
7	175	7525	120	40	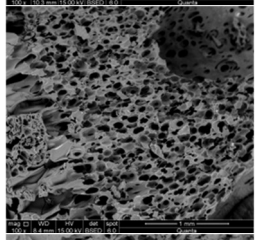	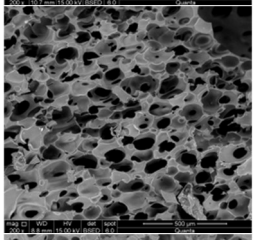	136.47	143.98	2.40E+06
8	175	7525	200	40	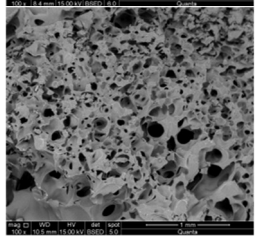	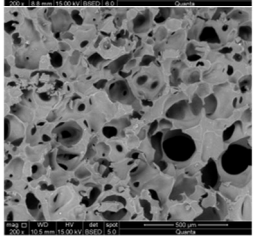	124.07	61.11	1.08E+06

Table 3 (cont.). Runs, experimental impregnation conditions, SEM imagess, cells diameter, standard deviations and cells density.

Run	Gemcitabine (mg GEM/ g PLGA)	Ratio PLA:PGA	Pres. (bar)	Temp. (°C)	SEM images 100x	SEM images 200x	Cell diameter (µm)	Stand. Deviation (µm)	Cell density (cells/cm³)
9	105	5050	120	25	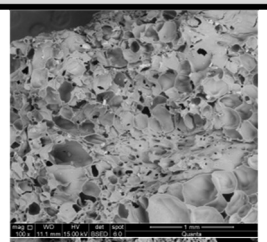	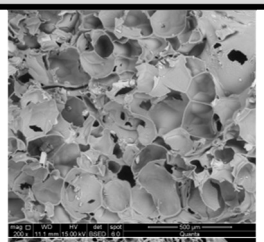	152.24	113.59	1.04E+06
10	105	5050	200	25	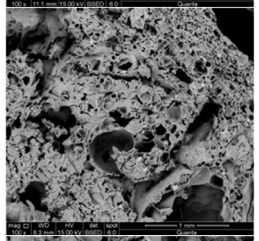	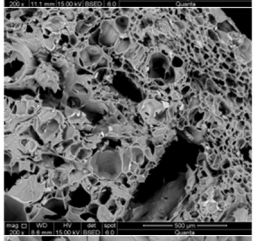	85.52	123.21	4.12E+06
11	105	5050	120	40	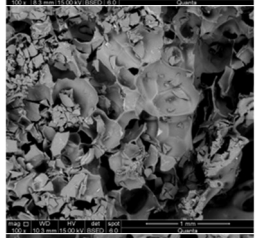	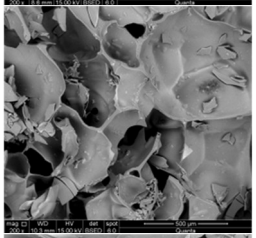	Non homogeneous foam		
12	105	5050	200	40	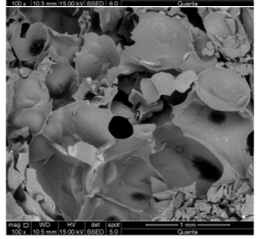	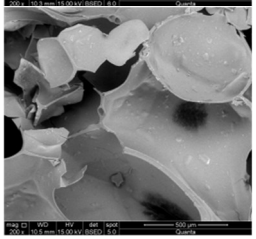	Non homogeneous foam		

Table 3 (cont.). Runs, experimental impregnation conditions, SEM imagess, cells diameter, standard deviations and cells density.

Run	Gemcitabine (mg GEM/ g PLGA)	Ratio PLA:PGA	Pres. (bar)	Temp. (°C)	SEM images 100x	SEM images 200x	Cell diameter (µm)	Stand. Deviation (µm)	Cell density (cells/cm³)
13	105	7525	120	25	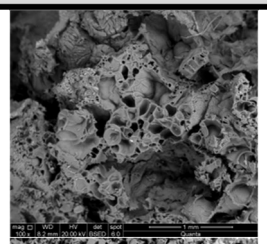	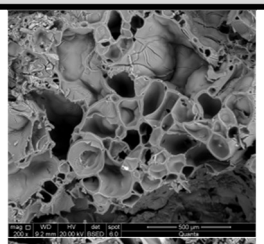	Non homogeneous foam		
14	105	7525	200	25	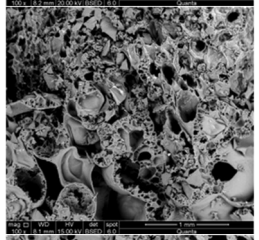	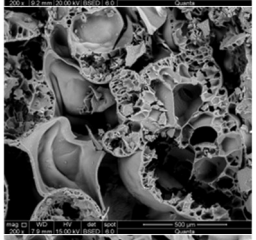	Non homogeneous foam		
15	105	7525	120	40	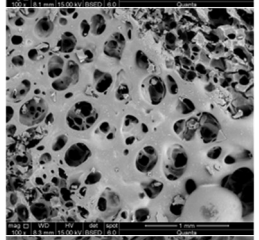	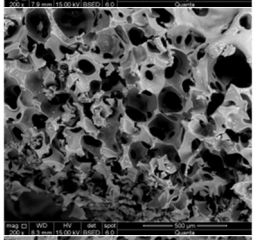	130.08	87.76	7.99E+05
16	105	7525	200	40	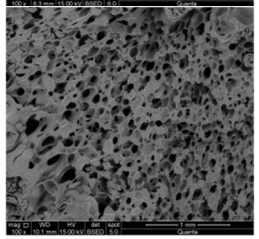	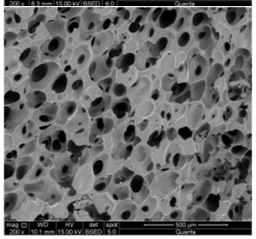	129.93	44.12	2.10E+06

Table 3 (cont.). Runs, experimental impregnation conditions, SEM imagess, cells diameter, standard deviations and cells density.

Run	Gemcitabine (mg GEM/ g PLGA)	Ratio PLA:PGA	Pres. (bar)	Temp. (°C)	SEM images 100x	SEM images 200x	Cell diameter (µm)	Stand. Deviation (µm)	Cell density (cells/cm³)
17	35	5050	120	25	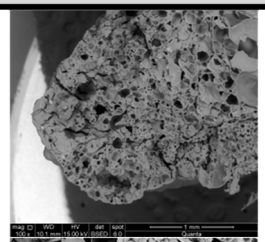	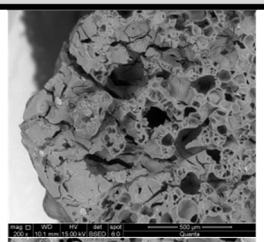	88.57	82.77	1.32E+06
18	35	5050	200	25	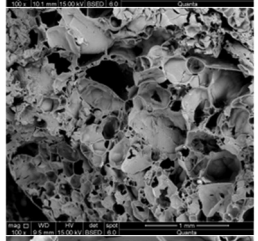	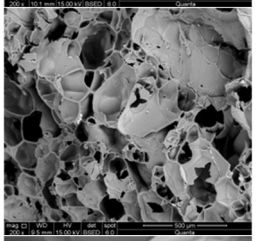	158.91	148.18	1.99E+06
19	35	5050	120	40	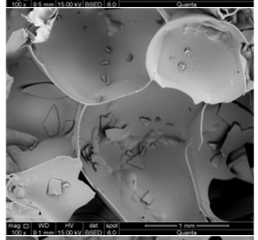	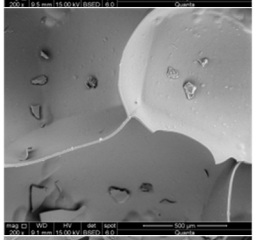	Non homogeneous foam		
20	35	5050	200	40	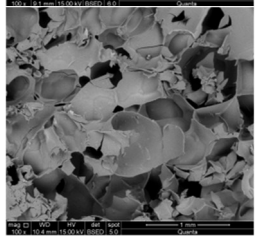	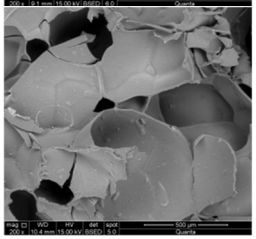	Non homogeneous foam		

Table 3 (cont.). Runs, experimental impregnation conditions, SEM imagess, cells diameter, standard deviations and cells density.

Run	Gemcitabine (mg GEM/ g PLGA)	Ratio PLA:PGA	Pres. (bar)	Temp. (°C)	SEM images 100x	SEM images 200x	Cell diameter (µm)	Stand. Deviation (µm)	Cell density (cells/cm³)
21	35	7525	120	25			Non homogeneous foam		
22	35	7525	200	25			Non homogeneous foam		
23	35	7525	120	40			90.50	43.09	4.79E+06
24	35	7525	200	40			153.59	110.97	8.16E+05

For a better observation of the results obtained, Figure 1 represents the cell diameter together with the standard deviation, as well as the density of cells for each run. The four graphs that make up this Figure represent the value of the variables studied for the same lactide:glycolide ratio and operating pressure. Experiments in which the internal structure of the foam did not show a homogeneous distribution were discarded as they may result in different drug release rates. In this way, a controlled release in time would not be achieved and could cause undesirable side effects.

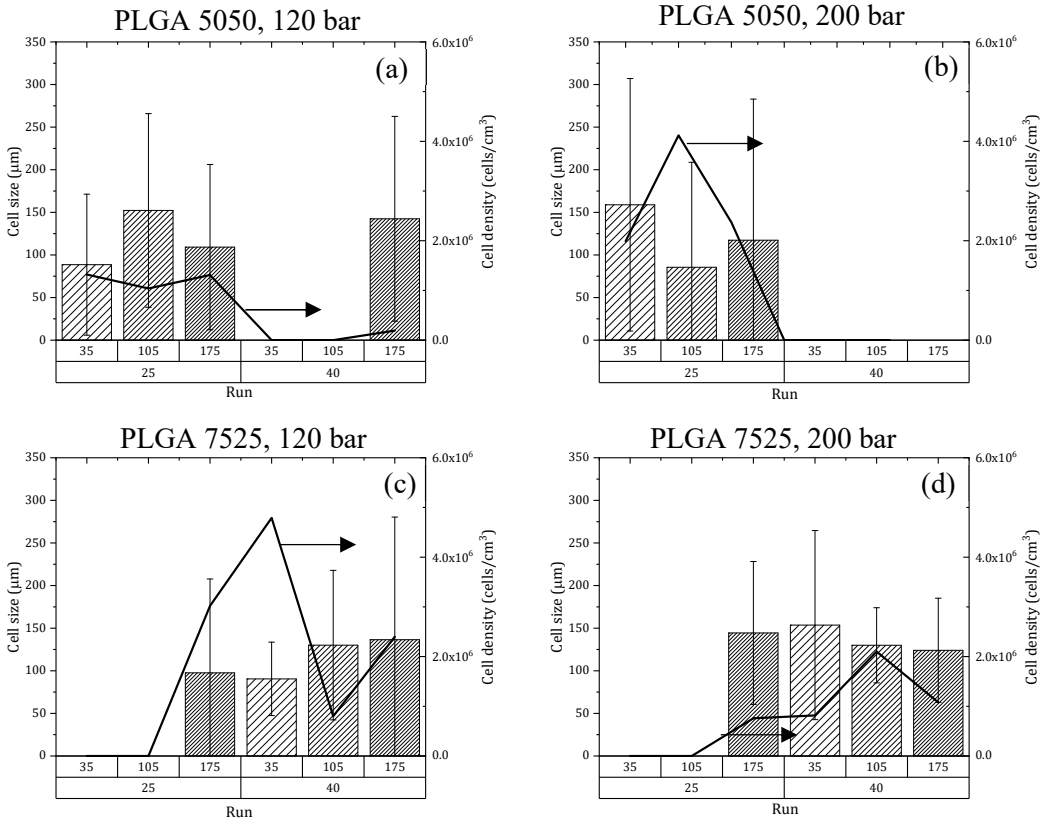

Figure 1. Comparison of the obtained cell size, standard deviation (columns, left axis) and cell density (line, right axis) for experiments performed under the same conditions for the three different Gemcitabine/PLGA ratios.

In view of the results obtained, the addition of the drug caused the cell size to be greatly reduced compared to previous experiments. This phenomenon may be caused because Gemcitabine crystals act as nucleating agents. Gutiérrez et al. [44] demonstrated a significant effect on the homogeneity of cell size distribution due to the presence of nanoparticles. The

286 addition of these nanoparticles in the foaming of polystyrene solutions resulted in a decrease in
287 particle size compared to experiments without nucleating agents. Higher nucleation rate was
288 observed at higher concentration and smaller size of nanoparticles because of a decrease in the
289 interfacial tension. In this investigation, the addition of Gemcitabine resulted in a higher number
290 of nucleation sites and a higher nucleation was achieved compared to foams that did not contain
291 the drug. Cell density increased to $2 \cdot 10^6$ cells/cm^3 in the impregnation experiments. This effect
292 was also confirmed by Xin et al. [53] by using bioactive particles for osteogenesis as nucleation
293 agents.

294 Concerning the effect of the ratio PLA to PGA, pressure and temperature on the cell size,
295 a unique pattern could not be established. Cell size of the foams varied between 35 µm and 158
296 µm, reaching the highest cell density for experiment 23. In this experiment, Gemcitabine
297 concentration was 35 mg Gemcitabine/g PLGA, at 120 bar and 40 °C. This foam presented an
298 excellent, smooth and uniform structure due to the homogeneous dispersion of the drug.

299

300 **b) Impregnation efficiency analysis**

301 Impregnation efficiency is a key parameter since the optimum amount of Gemcitabine in
302 the foams should be optimised. As can be seen in Table 4, for all experiments, an impregnation
303 efficiency of over 88% was achieved. Previous experiments demonstrated the insolubility of
304 Gemcitabine in CO_2. Thus, a poor dispersion of the drug in the polymeric matrix could be
305 expected, but the use of homogeneous dispersions of Gemcitabine in PLGA-ethyl lactate
306 solutions facilitates a uniform impregnation.

307

308

309

310

311

312

313

314 Table 4. Impregnation efficiency of Gemcitabine foams for each experimental run.

Run	Drug loading (mg GEM/ g PLGA)	Ratio PLA:PGA	Pres. (bar)	Temp. (°C)	Impregnation Efficiency (%)
1	175	5050	120	25	96.70
2	175	5050	200	25	95.21
3	175	5050	120	40	91.10
4	175	5050	200	40	95.17
5	175	7525	120	25	99.44
6	175	7525	200	25	92.87
7	175	7525	120	40	93.54
8	175	7525	200	40	91.20
9	105	5050	120	25	97.00
10	105	5050	200	25	93.74
11	105	5050	120	40	97.45
12	105	5050	200	40	98.31
13	105	7525	120	25	93.60
14	105	7525	200	25	95.44
15	105	7525	120	40	95.18
16	105	7525	200	40	94.85
17	35	5050	120	25	98.36
18	35	5050	200	25	97.65
19	35	5050	120	40	97.24
20	35	5050	200	40	93.56
21	35	7525	120	25	88.03
22	35	7525	200	25	92.20
23	35	7525	120	40	94.98
24	35	7525	200	40	91.33

315

316

317 An analysis of the foams was also carried out using the "Energy Dispersive Spectroscopy"
318 (EDS) system, which makes it possible to identify the elements that compose a sample and their
319 relative proportions. As an example, the Table 5 shows the results obtained with this technique
320 for run 1 (120 bar, 25 °C, ratio PLA to PGA 50:50, initial drug loading 175 mg GEM/g PLGA).
321 The first black and white photograph shows the SEM analysis for the foam. The coloured
322 photographs, on the other hand, were a mapping of the black-and-white photograph where each
323 colour corresponded to a compound. Carbon (red) and Oxygen (blue) gave rise to a greater
324 coloration since they are the compounds that mainly compose both the structure of PLGA and
325 Gemcitabine. It was for this reason that it was necessary to identify the characteristic elements of
326 the drug in order to be able to differentiate it from the polymer. Considering the structure of
327 Gemcitabine, these elements were Fluorine (yellow), Nitrogen (green) and Chlorine (purple). The
328 presence of Chlorine in the structure was due to the fact that the compound used was Gemcitabine

Hydrochloride. Attending to these three photographs, the coloration appears distributed through all the interior of the foams. This indicated that the drug inside will only be released into the medium when the foam degrades, resulting in a controlled release over time.

Table 5. EDS analysis for Run 1. Each colour corresponds to one element present in the internal structure of the foam.

SEM image for Run 1				
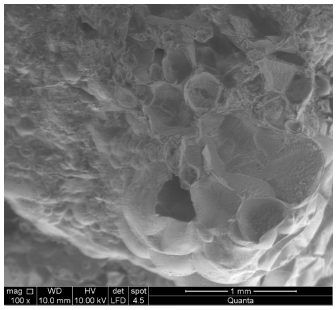				
Elements				
Carbon	**Oxygen**	**Fluorine**	**Nitrogen**	**Chlorine**
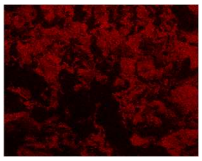	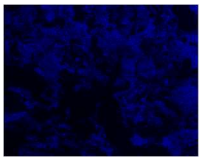	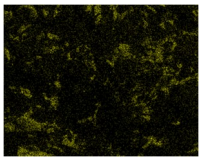	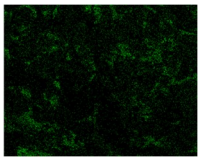	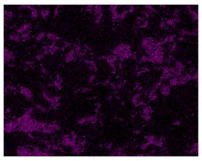

The presence of Gemcitabine in the foams was further confirmed by infrared analysis of the samples. The spectra of PLGA polymer, Gemcitabine, non-impregnated foam and impregnated foam are shown in Figure 2.

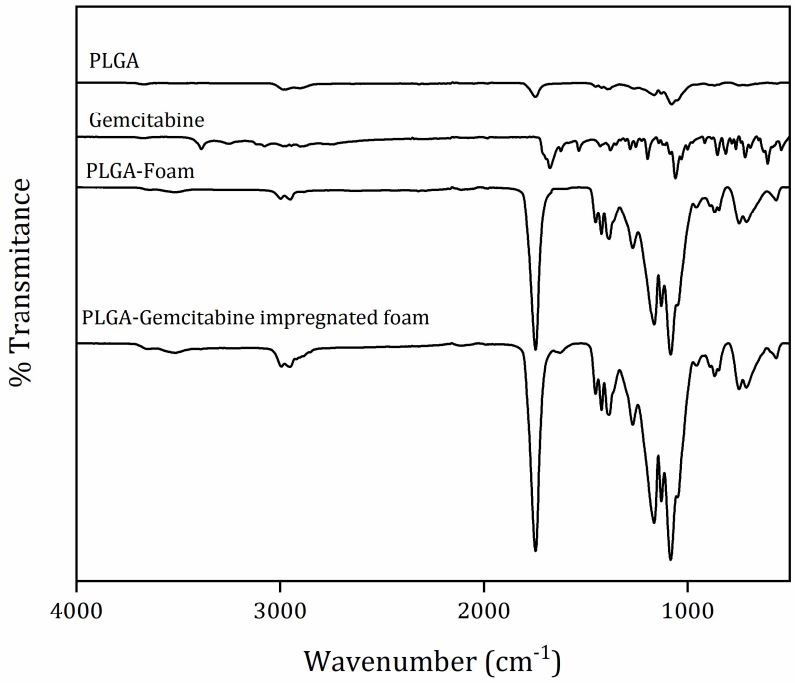

Figure 2. FTIR spectra of PLGA polymer, Gemcitabine, PLGA foam and PLGA-Gemcitabine impregnated foam.

In the FTIR spectra of PLGA polymer, the peak at 1750 cm^{-1} corresponded to the absorbance of carbonyl group in PLGA matrix, and peaks at 2991 cm^{-1} and 2952 cm^{-1} corresponded to C-H bending vibrations. The FTIR of Gemcitabine showed at 1700 cm^{-1} and 1679 cm^{-1} the bending vibrations of amines and the amine one at 3256 cm^{-1}. The spectrum of Gemcitabine-impregnated foams exhibited the peak of carbonyl group C=O at 1750 cm^{-1}, which was not found in pure polymer. After impregnation process, this peak appeared in the same position indicating the correct impregnation of the drug into the polymer matrix [26, 54]. C-H bending vibrations were present at 2998 cm^{-1} and 2946 cm^{-1}. The peak at 1633 cm^{-1} reinforced the presence of amide bond. These results were in agreement with previous researches in the formation of PLGA-Gemcitabine conjugates [40, 55-58].

356 **c) Thermal analysis**

357 Table 6 shows the residual amount of solvent present in the foams after depressurization
358 as well as the glass transition temperature.

359 Table 6. Residual amount of solvent in the foams and glass transition temperature for each run.

Run	Drug loading (mg GEM/ g PLGA)	Ratio PLA:PGA	Pres. (bar)	Temp. (°C)	Residual solvent (%)	Tg (°C)
1	175	5050	120	25	1.51	40.21
2	175	5050	200	25	1.65	39.65
3	175	5050	120	40	2.03	38.24
4	175	5050	200	40	2.99	39.14
5	175	7525	120	25	0.30	41.23
6	175	7525	200	25	1.87	40.25
7	175	7525	120	40	2.78	39.65
8	175	7525	200	40	2.22	39.40
9	105	5050	120	25	1.15	41.78
10	105	5050	200	25	1.47	40.56
11	105	5050	120	40	3.69	38.98
12	105	5050	200	40	2.01	39.54
13	105	7525	120	25	0.76	39.81
14	105	7525	200	25	0.55	40.36
15	105	7525	120	40	1.49	40.21
16	105	7525	200	40	1.88	38.88
17	35	5050	120	25	0.78	39.69
18	35	5050	200	25	0.43	39.82
19	35	5050	120	40	0.97	40.12
20	35	5050	200	40	1.87	41.05
21	35	7525	120	25	0.66	40.36
22	35	7525	200	25	0.64	40.87
23	35	7525	120	40	3.01	39.61
24	35	7525	200	40	3.33	40.41

360

361 TGA analysis carried out to determine the residual amount of solvent showed the peak
362 decomposition of Gemcitabine as can be seen in Figure 3. The amount of solvent present in the
363 foams was measured and did not exceed 4% in all of them. At 145 °C the degradation peak
364 corresponding to residual ethyl lactate can be observed. The degradation peak of Gemcitabine
365 was found at 280 °C, confirming again the presence of the drug. Finally, the peak for PLGA
366 degradation appears at 325 °C, temperature at which the maximum slope of degradation is
367 displayed.

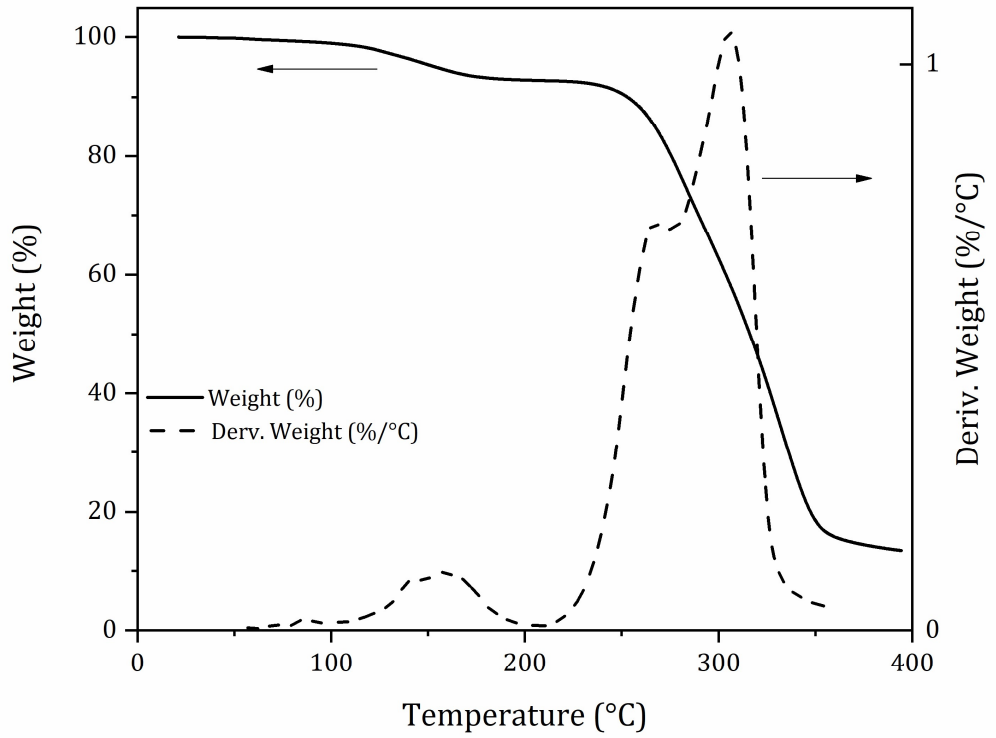

Figure 3. TGA analysis of an impregnated foam using the software TA Universal. The degradation peaks corresponding to ethyl lactate, Gemcitabine and polymer are shown.

DSC analysis of impregnated foams is shown in Figure 4. It confirmed that the glass transition temperature did not vary significantly over the initial one of the polymer, thus remaining above body temperature and confirming that it is suitable for its use as drug delivery system. Its average value was about 40 °C considering all the experiments. This value is above body temperature which is another indication that these Gemcitabine impregnated PLGA foams can be used as controlled release systems.

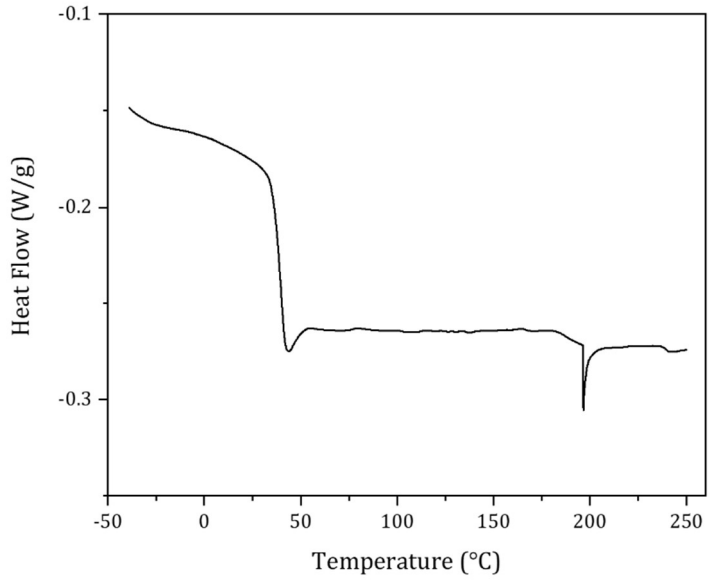

Figure 4. Second heating in the DSC analysis of a Gemcitabine impregnated foam.

3.2. *In vitro* drug release experiments

The *in vitro* process of drug release from the foam to an aqueous medium (Phosphate Buffered Saline) was studied. The study of the release kinetics of a drug that is occluded within a release system is highly important for the development of these systems, as it provides knowledge of the mechanism by which the release process occurs. Generally, the drug is distributed in the polymeric matrix and is released by two fundamental mechanisms: diffusion through the matrix and degradation of the polymer, which leads to erosion of the foam.

Figure 5 shows the release curves for runs 1, 5, 9, 13, 17 and 21. These experiments were selected since under these conditions a good impregnation of the drug in the polymeric matrix was obtained. In addition, working at lower pressures and temperatures avoids a possible degradation of the active ingredient. Next, the effect of Gemcitabine concentration and composition of polymer matrix was studied on the drug release.

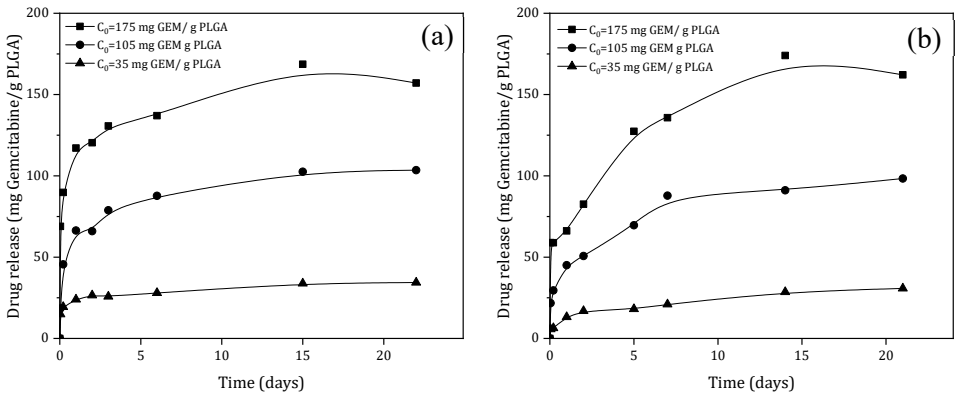

Figure 5. Experimental data for Gemcitabine release at three different concentrations Gemcitabine/PLGA. (a) PLGA5050 and (b) PLGA7525. (■) C_0= 175 mg Gemcitabine/g PLGA, (●) C_0= 105 mg Gemcitabine/g PLGA, (▲) C_0= 35 mg Gemcitabine/g PLGA.

Figure 5 shows a relationship between the shape of the curves and the drug loading of the foams. An increase in the rate of release of Gemcitabine occurs at higher initial concentrations of the drug in the foam. This may be due to increased deposition of the drug on the surface of the foam, making its release into the medium faster.

Although experiments 17 (Experimental conditions: C_0 = 105 mg GEM/g PLGA, PLGA7525, 120 bar and 25 °C) and 21 (Experimental conditions: C_0 = 35 mg GEM/g PLGA, PLGA7525, 120 bar and 25 °C) did not present a homogeneous internal structure, their liberation profile was also studied to determine whether this lack of homogeneity conditioned the release rate. According to the release profiles, no significant variation or appearance of different release ratios was observed whereas in the case of experiment 21, the lowest impregnation efficiency is obtained.

Regarding the PLA to PGA ratio of the polymer, many authors state it as the most important factor that determines the release rate of the drug [10, 45, 59-62]. The presence of glycolide in the polymer increases its degradation rate [7, 63] since a higher content of glycolide makes the polymer more hydrophilic than PLA and increases more pronounced polymer swelling

due to the best penetration of water molecules between the polymer chains [64]. Slower degradation and release rate was observed in Figure 6.b for the foams synthetized using PLGA7525 as the polymer either the loading of Gemcitabine.

3.3. Model fitting

Finally, experimental data were fitted using a mathematical model, which stablished the release kinetics of Gemcitabine depending on the composition of the polymer and the drug loading. Figure 6 shows this fit of experiment data for the three different release zones. Table 7 summarizes the fitted data for the model parameters defined in previous section.

Table 7. Fitted values for parameters of the proposed model: (a) PLGA5050, (b) PLGA7525.

(a) PLGA5050

	k_{ext} (h^{-1})	D (cm^2/s)	k_{deg} (cm)
175 mg GEM/g PLGA	0.138	4.33E-07	0.021
105 mg GEM/g PLGA	0.029	2.25E-07	0.019
35 mg GEM/g PLGA	0.153	4.89E-07	0.018

(b) PLGA7525

	k_{ext} (h^{-1})	D (cm^2/s)	k_{deg} (cm)
175 mg GEM/g PLGA	0.054	2.84E-07	0.014
105 mg GEM/g PLGA	0.025	2.50E-07	0.013
35 mg GEM/g PLGA	0.015	1.36E-07	0.013

In Figure 6 the three different zones of the proposed model are separated by a vertical dashed line at t = 1 day (Zone I and II separation) and t = 5 days (Zone II and III separation).

As commented in the previous section, the initial part of the release curves (Zone I) would correspond with the external mass transfer process. The fitted values for k_{ext} were ranged from 0.15 h^{-1} for PLGA5050 at the highest drug loading to 0.015 h^{-1} for PLGA7525 at the lowest drug loading, thus confirming that a decrease in the drug loading in the polymeric matrix resulted in lower release rates.

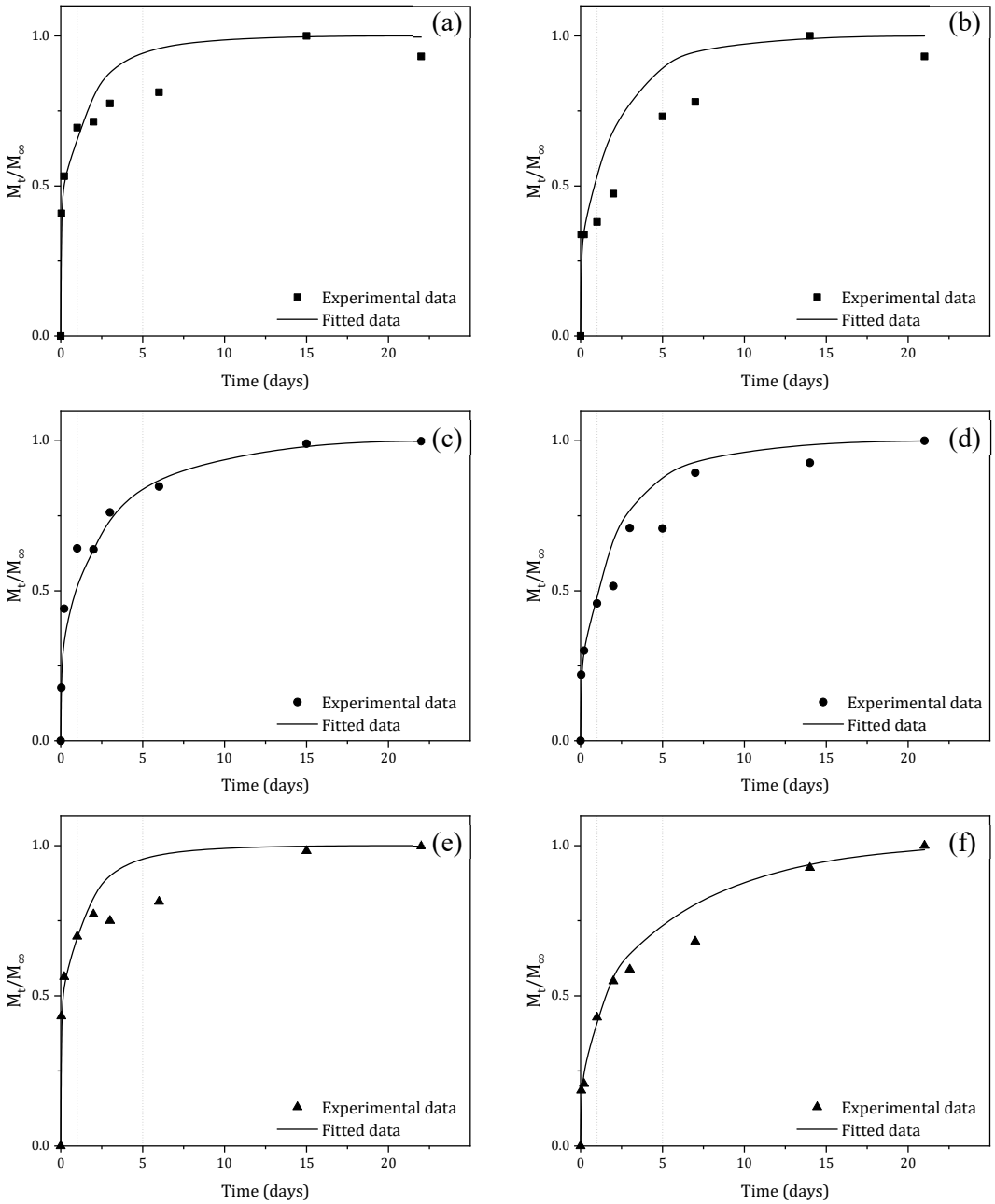

Figure 6. Cumulative Gemcitabine release profiles using PLGA5050 and PLGA 7525 under different drug loading. Symbols show the experimental data and curves are the theoretical values calculated for the zones I, II and III respectively. (a) PLGA5050, 175 mg Gemcitabine/g PLGA, (b) PLGA7525, 175 mg Gemcitabine/g PLGA, (c) PLGA5050, 105 mg Gemcitabine/g PLGA, (d) PLGA7525, 105 mg Gemcitabine/g PLGA, (e) PLGA5050, 35 mg Gemcitabine/g PLGA and (f) PLGA7525, 35 mg Gemcitabine/g PLGA.

447 As can be appreciated in the graphs, when k_{ext} increased, the burst was more pronounced
448 what means that the drug was initially more rapidly released. The increase in the amount of
449 glycolide in the composition of the polymer resulted in a higher degradation rate. For this reason,
450 in general, the values of k_{ext} under the same drug loading were higher in the case of PLGA5050
451 than in the case of PLGA7525.

452 For the Zone II, the diffusion values were in the range of 10^{-7} cm^2/s for all experiments.
453 Looking at Figure 6, it can be seen that the theoretical values did not fit well enough with the
454 experimental data at high initial concentrations of the drug. This may be due to the fact that the
455 high release of the drug at initial times caused an increase in apparent diffusivity promoting this
456 deviation. In addition, this model has been traditionally used for the adjustment of microparticles
457 and not for porous foams [65-67].

458 Finally, the adjustment of the experimental values for the polymer degradation constant
459 established that the highest degradation rates were obtained for PLGA5050 polymer at high
460 Gemcitabine loads due to the increased glycolide content.

461

462 # 4. Conclusions

463 Gemcitabine impregnation of PLGA polymeric matrices from its solution in ethyl lactate
464 has been performed for three different drug loading. In all experiments, cell size was in the range
465 of 35 µm to 158 µm. The presence of Gemcitabine was demonstrated by FTIR analysis and
466 because of the presence of its degradation peak in TGA analysis. The glass transition temperature
467 after the experiments did not vary from polymer flakes. Moreover, EDS analysis revealed a
468 homogeneous distribution of the drug throughout the internal structure of the foam.

469 The release kinetics of a hydrophilic drug such as Gemcitabine can be divided in three
470 steps. A first zone where the most accessible drug is released, a second zone where the diffusion
471 to the surface of the most inaccessible drug takes place and finally the degradation of the foam
472 and the release of the rest of Gemcitabine. The mathematical adjustment allowed calculating the

values of these constants. The higher values of k_{etx} and k_{deg} were obtained for the foams obtained with PLGA5050 containing the higher initial drug loading of Gemcitabine.

Acknowledgements

This work has been funded by the Spanish Ministry of Science and Innovation (CTQ2016-79811-P) and Junta de Castilla-La Mancha (PEII-2014-052-P), in part financed by the European Regional Development Fund (ERDF).

5. References

[1] Y. Ikada, H. Tsuji, Biodegradable polyesters for medical and ecological applications, Macromolecular rapid communications 21(3) (2000) 117-132

[2] I. Tsivintzelis, E. Pavlidou, C. Panayiotou, Biodegradable polymer foams prepared with supercritical CO2–ethanol mixtures as blowing agents, The Journal of Supercritical Fluids 42(2) (2007) 265-272 https://doi.org/10.1016/j.supflu.2007.02.009.

[3] C.M. Agrawal, R.B. Ray, Biodegradable polymeric scaffolds for musculoskeletal tissue engineering, Journal of Biomedical Materials Research: An Official Journal of The Society for Biomaterials, The Japanese Society for Biomaterials, and The Australian Society for Biomaterials and the Korean Society for Biomaterials 55(2) (2001) 141-150

[4] T.A. Holland, A.G. Mikos, Biodegradable polymeric scaffolds. Improvements in bone tissue engineering through controlled drug delivery, Tissue Engineering I, Springer2005, pp. 161-185.

[5] F. Mohamed, C.F. van der Walle, Engineering biodegradable polyester particles with specific drug targeting and drug release properties, Journal of pharmaceutical sciences 97(1) (2008) 71-87 10.1002/jps.21082.

[6] L.R. Jaidev, U.M. Krishnan, S. Sethuraman, Gemcitabine loaded biodegradable PLGA nanospheres for in vitro pancreatic cancer therapy, Materials science & engineering. C, Materials for biological applications 47 (2015) 40-7 10.1016/j.msec.2014.11.027.

[7] H.K. Makadia, S.J. Siegel, Poly Lactic-co-Glycolic Acid (PLGA) as Biodegradable Controlled Drug Delivery Carrier, Polymers 3(3) (2011) 1377-1397 10.3390/polym3031377.

[8] H.R. Lin, C.J. Kuo, C.Y. Yang, S.Y. Shaw, Y.J. Wu, Preparation of macroporous biodegradable PLGA scaffolds for cell attachment with the use of mixed salts as porogen additives, Journal of Biomedical Materials Research 63(3) (2002) 271-279 10.1002/jbm.10183.

[9] D.H. Lewis, Controlled release of bioactive agents from lactide/glycolide polymers, Biodegradable polymers as drug delivery systems. (1990) 1-41

[10] A. Göpferich, Mechanisms of polymer degradation and erosion, Biomaterials 17(2) (1996) 103-114

[11] S. Milovanovic, D. Markovic, A. Mrakovic, R. Kuska, I. Zizovic, S. Frerich, J. Ivanovic, Supercritical CO2 - assisted production of PLA and PLGA foams for controlled thymol release, Materials Science and Engineering: C 99 (2019) 394-404 https://doi.org/10.1016/j.msec.2019.01.106.

[12] D.D. Hile, M.L. Amirpour, A. Akgerman, M.V. Pishko, Active growth factor delivery from poly(D,L-lactide-co-glycolide) foams prepared in supercritical CO<inf>2</inf>, Journal of Controlled Release 66(2-3) (2000) 177-185 10.1016/S0168-3659(99)00268-0.

[13] C. Forest, P. Chaumont, P. Cassagnau, B. Swoboda, P. Sonntag, Polymer nano-foams for insulating applications prepared from CO2 foaming, Progress in Polymer Science 41 (2015) 122-145 https://doi.org/10.1016/j.progpolymsci.2014.07.001.
[14] S.L. Ishaug, G.M. Crane, M.J. Miller, A.W. Yasko, M.J. Yaszemski, A.G. Mikos, Bone formation by three-dimensional stromal osteoblast culture in biodegradable polymer scaffolds, J Biomed Mater Res 36(1) (1997) 17-28
[15] C.E. Holy, S.M. Dang, J.E. Davies, M.S. Shoichet, In vitro degradation of a novel poly(lactide-co-glycolide) 75/25 foam, Biomaterials 20(13) (1999) 1177-85
[16] A.R.C. Duarte, J.F. Mano, R.L. Reis, Preparation of chitosan scaffolds loaded with dexamethasone for tissue engineering applications using supercritical fluid technology, European Polymer Journal 45(1) (2009) 141-148 https://doi.org/10.1016/j.eurpolymj.2008.10.004.
[17] A.R.C. Duarte, S.G. Caridade, J.F. Mano, R.L. Reis, Processing of novel bioactive polymeric matrixes for tissue engineering using supercritical fluid technology, Materials Science and Engineering: C 29(7) (2009) 2110-2115 https://doi.org/10.1016/j.msec.2009.04.012.
[18] C.A. García-González, A.R.S.d. Sousa, A. Argemí, A.L. Periago, J. Saurina, C.M.M. Duarte, C. Domingo, Production of hybrid lipid-based particles loaded with inorganic nanoparticles and active compounds for prolonged topical release, International Journal of Pharmaceutics 382(1) (2009) 296-304 https://doi.org/10.1016/j.ijpharm.2009.08.033.
[19] A.R.C. Duarte, J.F. Mano, R.L. Reis, Supercritical fluids in biomedical and tissue engineering applications: a review, International Materials Reviews 54(4) (2009) 214-222 10.1179/174328009X411181.
[20] B.D. Ratner, A.S. Hoffman, F.J. Schoen, J.E. Lemons, Biomaterials science: an introduction to materials in medicine, Elsevier2004.
[21] B.D. Ratner, Biomaterials: Been There, Done That, and Evolving into the Future, Annual Review of Biomedical Engineering 21(1) (2019) 171-191 10.1146/annurev-bioeng-062117-120940.
[22] I. García-Casas, C. Crampon, A. Montes, C. Pereyra, E.M. de La Ossa, E. Badens, Supercritical CO2 impregnation of silica microparticles with quercetin, The Journal of Supercritical Fluids 143 (2019) 157-161
[23] S. Freiberg, X. Zhu, Polymer microspheres for controlled drug release, International journal of pharmaceutics 282(1-2) (2004) 1-18
[24] A.R.C. Duarte, T. Casimiro, A. Aguiar-Ricardo, A.L. Simplício, C.M.M. Duarte, Supercritical fluid polymerisation and impregnation of molecularly imprinted polymers for drug delivery, The Journal of Supercritical Fluids 39(1) (2006) 102-106 https://doi.org/10.1016/j.supflu.2006.01.013.
[25] L.I. Cabezas, I. Gracia, M.T. García, A. De Lucas, J.F. Rodríguez, Production of biodegradable porous scaffolds impregnated with 5-fluorouracil in supercritical CO<inf>2</inf>, Journal of Supercritical Fluids 80 (2013) 1-8 10.1016/j.supflu.2013.03.030.
[26] L.I. Cabezas, V. Fernández, R. Mazarro, I. Gracia, A. De Lucas, J.F. Rodríguez, Production of biodegradable porous scaffolds impregnated with indomethacin in supercritical CO<inf>2</inf>, Journal of Supercritical Fluids 63 (2012) 155-160 10.1016/j.supflu.2011.12.002.
[27] R. Campardelli, P. Franco, E. Reverchon, I. De Marco, Polycaprolactone/nimesulide patches obtained by a one-step supercritical foaming + impregnation process, The Journal of Supercritical Fluids 146 (2019) 47-54 https://doi.org/10.1016/j.supflu.2019.01.008.
[28] A.A. Barros, J.M. Silva, R. Craveiro, A. Paiva, R.L. Reis, A.R.C. Duarte, Green solvents for enhanced impregnation processes in biomedicine, Current Opinion in Green and Sustainable Chemistry 5 (2017) 82-87 https://doi.org/10.1016/j.cogsc.2017.03.014.
[29] A.R.C. Duarte, A.L. Simplicio, A. Vega-González, P. Subra-Paternault, P. Coimbra, M. Gil, H.C. de Sousa, C.M. Duarte, Supercritical fluid impregnation of a biocompatible polymer for ophthalmic drug delivery, The Journal of supercritical fluids 42(3) (2007) 373-377
[30] A. Hilbig, H. Oettle, Gemcitabine in the treatment of metastatic pancreatic cancer, Expert Review of Anticancer Therapy 8(4) (2008) 511-523 10.1586/14737140.8.4.511.

[31] A.G. Favaretto, Non-platinum combination of gemcitabine in NSCLC, Annals of oncology : official journal of the European Society for Medical Oncology 17 Suppl 5 (2006) v82-5 10.1093/annonc/mdj957.
[32] D. Lorusso, A. Di Stefano, F. Fanfani, G. Scambia, Role of gemcitabine in ovarian cancer treatment, Annals of oncology : official journal of the European Society for Medical Oncology 17 Suppl 5 (2006) v188-94 10.1093/annonc/mdj979.
[33] S. Dent, H. Messersmith, M. Trudeau, Gemcitabine in the management of metastatic breast cancer: A systematic review, Breast Cancer Research and Treatment 108(3) (2008) 319-331 10.1007/s10549-007-9610-z.
[34] H. Burris, A.M. Storniolo, Assessing clinical benefit in the treatment of pancreas cancer: gemcitabine compared to 5-fluorouracil, European journal of cancer (Oxford, England : 1990) 33 Suppl 1 (1997) S18-22
[35] S. Allison Logan, A.J. Brissenden, M.R. Szewczuk, R.J. Neufeld, Combinatorial and sequential delivery of gemcitabine and oseltamivir phosphate from implantable poly(D,L-lactic-co-glycolic acid) cylinders disables human pancreatic cancer cell survival, Drug Design, Development and Therapy 11 (2017) 2239-2250 10.2147/DDDT.S137934.
[36] J. Zhou, J. Wang, Q. Xu, S. Xu, J. Wen, Z. Yu, D. Yang, Folate-chitosan-gemcitabine core-shell nanoparticles targeted to pancreatic cancer, Chinese Journal of Cancer Research 25(5) (2013) 527-535 10.3978/j.issn.1000-9604.2013.09.04.
[37] D. Cosco, A. Bulotta, M. Ventura, C. Celia, T. Calimeri, G. Perri, D. Paolino, N. Costa, P. Neri, P. Tagliaferri, P. Tassone, M. Fresta, In vivo activity of gemcitabine-loaded PEGylated small unilamellar liposomes against pancreatic cancer, Cancer Chemotherapy and Pharmacology 64(5) (2009) 1009-1020 10.1007/s00280-009-0957-1.
[38] G. Birhanu, H.A. Javar, E. Seyedjafari, A. Zandi-Karimi, Nanotechnology for delivery of gemcitabine to treat pancreatic cancer, Biomedicine & Pharmacotherapy 88 (2017) 635-643 https://doi.org/10.1016/j.biopha.2017.01.071.
[39] C. Bornmann, R. Graeser, N. Esser, V. Ziroli, P. Jantscheff, T. Keck, C. Unger, U.T. Hopt, U. Adam, C. Schaechtele, U. Massing, E. Von Dobschuetz, A new liposomal formulation of Gemcitabine is active in an orthotopic mouse model of pancreatic cancer accessible to bioluminescence imaging, Cancer Chemotherapy and Pharmacology 61(3) (2008) 395-405 10.1007/s00280-007-0482-z.
[40] V. Khare, W.A. Sakarchi, P.N. Gupta, A.D.M. Curtis, C. Hoskins, Synthesis and characterization of TPGS–gemcitabine prodrug micelles for pancreatic cancer therapy, RSC Advances 6(65) (2016) 60126-60137 10.1039/C6RA09347G.
[41] C.R. Patra, R. Bhattacharya, E. Wang, A. Katarya, J.S. Lau, S. Dutta, M. Muders, S. Wang, S.A. Buhrow, S.L. Safgren, M.J. Yaszemski, J.M. Reid, M.M. Ames, P. Mukherjee, D. Mukhopadhyay, Targeted delivery of gemcitabine to pancreatic adenocarcinoma using cetuximab as a targeting agent, Cancer Research 68(6) (2008) 1970-1978 10.1158/0008-5472.CAN-07-6102.
[42] G.Y. Lee, W.P. Qian, L. Wang, Y.A. Wang, C.A. Staley, M. Satpathy, S. Nie, H. Mao, L. Yang, Theranostic nanoparticles with controlled release of gemcitabine for targeted therapy and MRI of pancreatic cancer, ACS Nano 7(3) (2013) 2078-2089 10.1021/nn3043463.
[43] J.-B. Bao, T. Liu, L. Zhao, G.-H. Hu, X. Miao, X. Li, Oriented foaming of polystyrene with supercritical carbon dioxide for toughening, Polymer 53(25) (2012) 5982-5993 https://doi.org/10.1016/j.polymer.2012.10.011.
[44] C. Gutiérrez, M.T. Garcia, R. Mencía, I. Garrido, J.F. Rodríguez, Clean preparation of tailored microcellular foams of polystyrene using nucleating agents and supercritical CO<inf>2</inf>, Journal of Materials Science 51(10) (2016) 4825-4838 10.1007/s10853-016-9776-z.
[45] L.I. Cabezas, I. Gracia, A. De Lucas, J.F. Rodríguez, Novel model for the description of the controlled release of 5-fluorouracil from PLGA and PLA foamed scaffolds impregnated in supercritical CO<inf>2</inf>, Industrial and Engineering Chemistry Research 53(40) (2014) 15374-15382 10.1021/ie404028t.

[46] G. Boyd, A. Adamson, L. Myers Jr, The exchange adsorption of ions from aqueous solutions by organic zeolites. II. Kinetics1, Journal of the American Chemical Society 69(11) (1947) 2836-2848

[47] J. Crank, The mathematics of diffusion, 347 pp, Clarendon Press, Oxford, 1956,

[48] O. Levenspiel, Chemical Reactor Omnibook-soft cover, Lulu. com2013.

[49] A.B. Nair, S. Jacob, A simple practice guide for dose conversion between animals and human, Journal of basic and clinical pharmacy 7(2) (2016) 27

[50] A.-A.K. Tentes, D. Kyziridis, S. Kakolyris, N. Pallas, G. Zorbas, O. Korakianitis, C. Mavroudis, N. Courcoutsakis, P. Prasopoulos, Preliminary results of hyperthermic intraperitoneal intraoperative chemotherapy as an adjuvant in resectable pancreatic cancer, Gastroenterology research and practice 2012 (2012)

[51] P.H. Sugarbaker, O.A. Stuart, L. Bijelic, Intraperitoneal gemcitabine chemotherapy treatment for patients with resected pancreatic cancer: rationale and report of early data, International journal of surgical oncology 2011 (2011)

[52] T.M. Cardillo, R. Blumenthal, Z. Ying, D.V. Gold, Combined gemcitabine and radioimmunotherapy for the treatment of pancreatic cancer, International journal of cancer 97(3) (2002) 386-392

[53] X. Xin, Y. Guan, S. Yao, Bi-/multi-modal pore formation of PLGA/hydroxyapatite composite scaffolds by heterogeneous nucleation in supercritical CO2 foaming, Chinese Journal of Chemical Engineering 26(1) (2018) 207-212 https://doi.org/10.1016/j.cjche.2017.04.005.

[54] Y. Kang, J. Wu, G. Yin, Z. Huang, Y. Yao, X. Liao, A. Chen, X. Pu, L. Liao, Preparation, characterization and in vitro cytotoxicity of indomethacin-loaded PLLA/PLGA microparticles using supercritical CO2 technique, European Journal of Pharmaceutics and Biopharmaceutics 70(1) (2008) 85-97

[55] X.-M. Tao, J.-c. Wang, J.-b. Wang, Q. Feng, S.-y. Gao, L.-R. Zhang, Q. Zhang, Enhanced anticancer activity of gemcitabine coupling with conjugated linoleic acid against human breast cancer in vitro and in vivo, European Journal of Pharmaceutics and Biopharmaceutics 82(2) (2012) 401-409 https://doi.org/10.1016/j.ejpb.2012.06.007.

[56] G. Cavallaro, L. Mariano, S. Salmaso, P. Caliceti, G. Gaetano, Folate-mediated targeting of polymeric conjugates of gemcitabine, International Journal of Pharmaceutics 307(2) (2006) 258-269 https://doi.org/10.1016/j.ijpharm.2005.10.015.

[57] V. Khare, S. Kour, N. Alam, R.D. Dubey, A. Saneja, M. Koul, A.P. Gupta, D. Singh, S.K. Singh, A.K. Saxena, P.N. Gupta, Synthesis, characterization and mechanistic-insight into the anti-proliferative potential of PLGA-gemcitabine conjugate, International Journal of Pharmaceutics 470(1-2) (2014) 51-62 10.1016/j.ijpharm.2014.05.005.

[58] Stevanovi, Magdalena, Radulovi, Aleksandra, Jordovi, Branka, Uskokovi, Dragan, Poly(DL-lactide-co-glycolide) Nanospheres for the Sustained Release of Folic Acid, Journal of Biomedical Nanotechnology 4(3) (2008) 349-358 10.1166/jbn.2008.321.

[59] L.I. Cabezas, I. Gracia, A. De Lucas, J.F. Rodríguez, Validation of a mathematical model for the description of hydrophilic and hydrophobic drug delivery from biodegradable foams: Experimental and comparison using indomethacin as released drug, Industrial and Engineering Chemistry Research 53(21) (2014) 8866-8873 10.1021/ie500760m.

[60] L. Lu, S.J. Peter, M. D. Lyman, H.L. Lai, S.M. Leite, J.A. Tamada, S. Uyama, J.P. Vacanti, L. Robert, A.G. Mikos, In vitro and in vivo degradation of porous poly(DL-lactic-co-glycolic acid) foams, Biomaterials 21(18) (2000) 1837-1845 10.1016/S0142-9612(00)00047-8.

[61] E. Markočič, T. Botić, S. Kavčič, T. Bončina, Z. Knez, In vitro degradation of poly(d, l -lactide- co -glycolide) foams processed with supercritical fluids, Industrial and Engineering Chemistry Research 54(7) (2015) 2114-2119 10.1021/ie504579y.

[62] C.E. LeBlon, R. Pai, C.R. Fodor, A.S. Golding, J.P. Coulter, S.S. Jedlicka, In vitro comparative biodegradation analysis of salt-leached porous polymer scaffolds, Journal of Applied Polymer Science 128(5) (2013) 2701-2712

[63] X.S. Wu, N. Wang, Synthesis, characterization, biodegradation, and drug delivery application of biodegradable lactic/glycolic acid polymers. Part II: biodegradation, Journal of biomaterials science. Polymer edition 12(1) (2001) 21-34

[64] L.Y. Lee, S.H. Ranganath, Y. Fu, J.L. Zheng, H.S. Lee, C.H. Wang, K.A. Smith, Paclitaxel release from micro-porous PLGA disks, Chemical Engineering Science 64(21) (2009) 4341-4349 10.1016/j.ces.2009.07.016.

[65] J. Siepmann, N. Faisant, J.-P. Benoit, A new mathematical model quantifying drug release from bioerodible microparticles using Monte Carlo simulations, Pharmaceutical research 19(12) (2002) 1885-1893

[66] D. Klose, F. Siepmann, K. Elkharraz, J. Siepmann, PLGA-based drug delivery systems: importance of the type of drug and device geometry, International journal of pharmaceutics 354(1-2) (2008) 95-103

[67] N. Faisant, J. Siepmann, J. Benoit, PLGA-based microparticles: elucidation of mechanisms and a new, simple mathematical model quantifying drug release, European Journal of Pharmaceutical Sciences 15(4) (2002) 355-366